

FMCW Radar-Based Human Activity Recognition: A Machine Learning Approach for Elderly Care

Original

FMCW Radar-Based Human Activity Recognition: A Machine Learning Approach for Elderly Care / Mashhadigholamali, Mohammadreza; Fard, Ali Samimi; Zolfaghari, Samaneh; Abedi, Hajar; Chakraborty, Mainak; Borzi, Luigi; Daneshtalab, Masoud; Shaker, George. - ELETTRONICO. - (2025), pp. 1-6. (IEEE Wireless Communications and Networking Conference (WCNC) Milan (Italy) 24–27 March 2025) [10.1109/wcnc61545.2025.10978639].

Availability:

This version is available at: 11583/3000127 since: 2025-06-19T20:11:36Z

Publisher:

IEEE

Published

DOI:10.1109/wcnc61545.2025.10978639

Terms of use:

This article is made available under terms and conditions as specified in the corresponding bibliographic description in the repository

Publisher copyright

IEEE postprint/Author's Accepted Manuscript

©2025 IEEE. Personal use of this material is permitted. Permission from IEEE must be obtained for all other uses, in any current or future media, including reprinting/republishing this material for advertising or promotional purposes, creating new collecting works, for resale or lists, or reuse of any copyrighted component of this work in other works.

(Article begins on next page)

FMCW Radar-Based Human Activity Recognition: A Machine Learning Approach for Elderly Care

Mohammadreza Mashhadigholamali¹ Ali Samimi Fard¹ Samaneh Zolfaghari² Hajar Abedi³
Mainak Chakraborty² Luigi Borzi¹ Masoud Daneshtalab² George Shaker³

¹ Department of Control and Computer Engineering, Politecnico di Torino, Turin, Italy.

Email: {mohammadreza.mashhadigholamali, ali.samimifard}@studenti.polito.it, luigi.borzi@polito.it

² School of Innovation, Design and Engineering, Mälardalen University, Västerås, Sweden.

Email: {samaneh.zolfaghari, mainak.chakraborty, masoud.daneshtalab}@mdu.se

³ Department of Electrical and Computer Engineering, University of Waterloo, Waterloo, Ontario, Canada.

Email: {habedifi, gshaker}@uwaterloo.ca

Abstract—In this paper, we propose a novel system prototype for human activity recognition using a low-cost, low-power millimeter-wave (mmWave) frequency-modulated continuous wave (FMCW) radar. Our approach applies the Fast Fourier Transform on the slow time axis and employs a Capon filter to generate range-Doppler, range-azimuth, and range-elevation maps, respectively. It can also effectively mitigate noise and multipath effects. We then use principal component analysis for feature reduction, reducing the dimensionality of the feature vectors extracted from these maps, which can be used to train conventional machine learning classifiers. This approach aims to achieve a balance between computational complexity, accuracy, and overall system performance. Our proposed system demonstrates promising recognition rates and robustness across varying levels of activity granularity, achieving recognition rates from 90.28% for four activities up to 70.97% for seven fine-grained activities. These findings highlight the potential of millimeter wave radar and suggested range maps combined with conventional machine learning classifiers for noninvasive, privacy-preserving activity recognition, with significant implications for healthcare, elderly care, and ambient assisted living.

Index Terms—mmWave, FMCW radar, human activity recognition, machine learning, deep learning, elderly care, ambient assisted living.

I. INTRODUCTION

Over the past decades, the increasing population of older adults has become a significant challenge for both developed and developing countries. By the end of the year 2050, about 22% of the world population is expected to be over 65 [1]. This demographic shift brings with it an increased prevalence of age-related diseases, necessitating continuous monitoring. Research suggests that timely and appropriate interventions could significantly reduce the number of fatal incidents and hospitalizations among older adults [2]. Consequently, there is a growing need for innovative ambient-assisted living (AAL) tools that leverage human activity recognition (HAR) to promote seniors' independent living. These tools also enable remote health monitoring aiding in rehabilitation, enhancing well-being, and detecting potential health issues early [3]–[5].

Recent advancements in sensor miniaturization, their integration into daily objects, and improvements in AI algorithms have considerably enhanced activity monitoring. These advancements enable the extraction of deeply hidden information

for more accurate detection and interpretation. Sensors used for HAR are broadly categorized into wearable and non-wearable sensors [3], [5].

In recent years, there has been a growing focus towards non-wearable due to their ability to collect activity data unobtrusively within the environment where activities occur [6]. While effective, non-wearable sensors face challenges, such as interference from external factors (e.g., sunlight or heat), limited detection range, maintenance requirements, and high deployment costs in diverse environments [5].

To address these limitations, radar-based sensors have emerged as a promising solution for in-home activity monitoring. Radar-based sensors offer advantages such as enhanced privacy, the ability to sense through walls and other obstacles, and functionality in low-light conditions [7], [8]. Radars are generally categorized into Continuous Wave (CW) radar and impulse radar, each with specific applications. Impulse radars are useful in vital signs detection, gesture recognition, and human tracking. While CW radar has been investigated for HAR in several studies, its inability to measure absolute range and range resolution poses significant challenges [9]–[11].

mmWave FMCW radar systems overcome many of these challenges by providing accurate subject localization and capturing micro-Doppler data. This makes them particularly suitable for in-home monitoring and recognizing a wide range of activities [7], [8]. In this study, we designed and developed a HAR framework using mmWave FMCW radar, focusing on the entire system architecture, including the radar setup, feature extraction, and processing pipeline, as well as carefully selected activities. Given the preliminary nature of our study and the unique contributions and data we focus on, it is challenging to compare our work with existing studies directly. Our work introduces a robust and efficient approach for activity recognition, with several distinct contributions compared to existing studies as follows.

- We designed and developed an end-to-end HAR framework with a carefully structured radar setup and preprocessing pipeline, extracting 3D data vectors to capture motion and spatial details, focusing on efficiency and

informativeness rather than conventional radar image-based processing.

- Unlike many studies in the literature, we focused on recognizing intricate, similar, and less-studied human activities that are more representative of real-life scenarios. To achieve this, we collected a radar dataset in a realistic environment specifically tailored to our use case.
- We proposed and implemented a fully functional, non-invasive HAR system prototype, showcasing its feasibility and practicality for real-world applications.
- We experimentally validated our prototype using conventional machine learning (ML) models, demonstrating its effectiveness and computational efficiency. Importantly, our contribution lies in the overall framework rather than the ML models' novelty.

The paper is structured as follows: Section II describes the methodology, including radar setup, data collection, and pre-processing. Section III presents the experimental analysis of ML classifiers performances. Section IV concludes with key findings and future work.

II. METHODOLOGY

In our work, we used a BGT60TR13C mmWave FMCW radar system from Infineon Technologies AG [12]. This radar operates by transmitting a sawtooth wave in the frequency range of 58 GHz to 63.5 GHz, utilizing one transmitter and three receivers. It features adjustable chirp duration and can measure azimuth, elevation, and target velocity. Based on the room structure, human walking speed, and the radar's inherent limitations, we configured the system with 128 samples per chirp and 128 chirps per frame to optimize the radar's maximum detectable range and velocity resolution. Detailed configuration and key parameters are listed in Table I. The antenna arrangement, shown in Fig. 1, is experimentally designed to ensure optimal coverage of the bedroom while minimizing side-lobe interference and maximizing performance. For signal processing, RX1 and RX3 antennas were utilized for azimuth calculations, while RX2 and RX3 were employed for elevation calculations in accordance with the specified arrangement.

TABLE I: Radar configuration and specification.

Parameters	Value
Radar Model	BGT60TR13C
Start Frequency	61 GHz
End Frequency	62 GHz
ADC Sampling Rate	2 Msps
Frame Rate	10
Chirps Per Frame	128
Number of Tx Antennas	1
Number of Rx Antennas	3
Range resolution	15 cm
Max Unambiguous Range	4.8 m

Fig. 2 illustrates an overview of the proposed system prototype for radar-based HAR. In the following sections we provide more detailed explanations of each module.

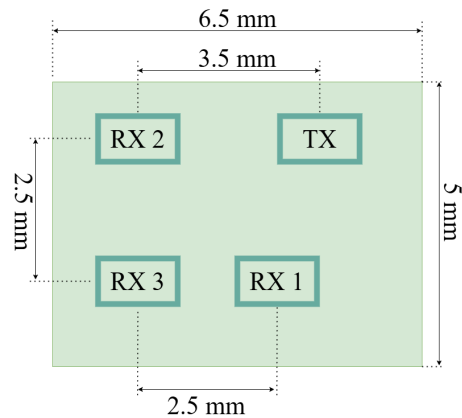


Fig. 1: BGT60TR13C top view and antenna arrangement.

A. Data Collection

To collect data, the radar was positioned at a height of 210 cm above the ground and angled at 30°. Three subjects (two male, one female) performed five activities across a total of 16 trials: two subjects completed six trials each, and one completed four. Each session began with 1 minute of empty-room data collection. Subjects then entered the room and walked for 2 minutes, sat on the bed for 2 minutes, lay on the bed for 5 minutes, and lay on the floor for another 5 minutes. They also sat on a chair for 2 minutes in some sessions. Transitional activities were grouped and labeled as “Transition”. Therefore, activities are classified into seven categories: Entering the room and walking, Sitting on the bed, Sitting on a chair, Lying on the bed, Lying on the floor, Empty room, and Transition. We have ensured that all necessary human concerns were addressed before collecting radar-based data. Additionally, the radar system used in this study is certified, ensuring compliance with relevant safety and ethical standards. Fig. 3a, and Fig. 3b, and Fig. 3c show examples of these activities.

In FMCW radars, a series of chirps is transmitted via the TX antenna, and each RX antenna captures the reflected signals. The collected data is organized into a radar data cube with dimensions $C \times N \times M$, where C represents the number of channels, N is the number of chirps per frame, and M is the number of samples per chirp. Each row, or *fast time*, contains signal samples within a single chirp, while each column, or *slow time*, represents the same sample position across multiple chirps [13]. This data structure facilitate feature extraction for detecting motion and spatial characteristics.

B. Preprocessing and Feature Extraction

For the preprocessing of collected data, spectral leakage in frequency domain signal processing was mitigated using the Blackman-Harris windowing function after removing DC bias [14]. The range of an object was then determined by applying the Fast Fourier Transform (FFT) along the fast time axis, with the peak of the spectrum indicating the object's distance, known as the range-FFT [15].

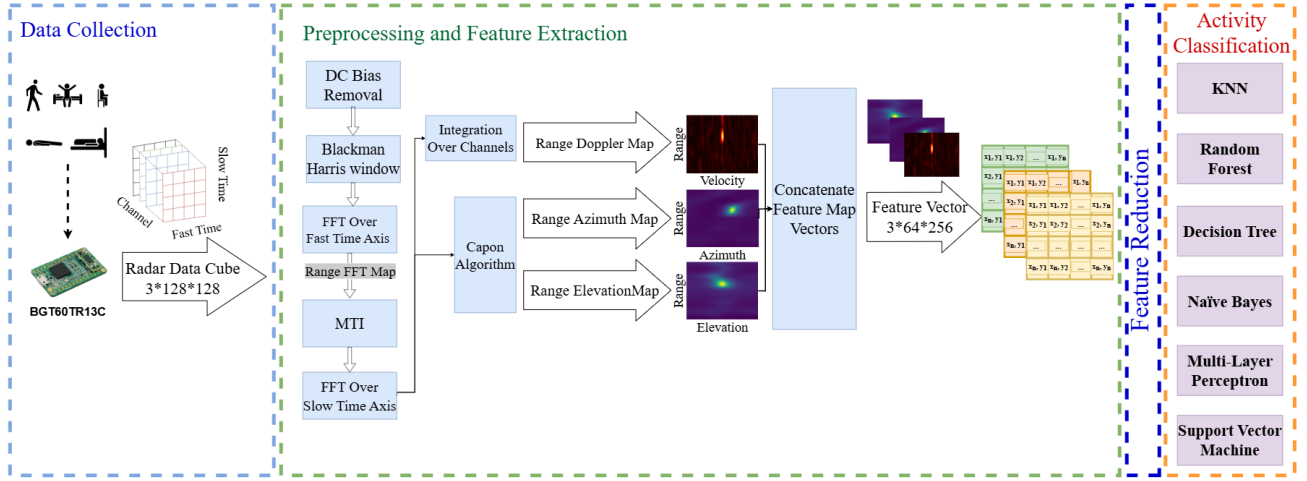


Fig. 2: Overview of the proposed system prototype of FMCW radar-based HAR.



(a) Lying on the floor.



(b) Sitting on chair.

(c) Lying on bed.

Fig. 3: An example of a subject performing activities in the room from radar's POV.

The remaining signal includes two reflection types: clutter from stationary objects (e.g., walls, floors, furniture) and reflections from moving people. To remove clutter, we used a Moving Target Indicator (MTI) algorithm, which employs linear filtering to reduce stationary reflections while preserving moving targets. At each time step, the peak value across slow time for each range bin, $r_{i,max}$, is combined with the previous MTI filter output t_{i-1} using a weighting factor α :

$$t_i = \alpha \cdot r_{i,max} + (1 - \alpha) \cdot t_{i-1} \quad (1)$$

At t_0 , the filter output t_i is initialized to zero. The MTI filter removes stationary clutter by subtracting t_{i-1} from $r_{i,max}$, yielding the filtered FFT value $r_{i,filt}$ [16]:

$$r_{i,filt} = |r_{i,max} - t_{i-1}| \quad (2)$$

This approach effectively eliminates stationary targets with minimal impact on slow-moving objects.

Next, a second FFT is applied along the slow time axis to obtain Doppler information for each channel, which is then integrated to create the range-Doppler map.

Moreover, multipath effects, where signals travel multiple routes and may be stronger than the actual reflected signal, can distort the range profile [17]. To accurately determine the subject's position and generate a precise range-azimuth and range-elevation map, we apply the Capon algorithm [8] to the range-Doppler map.

The Capon algorithm estimates the Angle of Arrival (AoA) by minimizing the output power P_{out} while ensuring a distortionless response at the desired angle. It is formulated as:

$$\min_{\mathbf{w}} \left(P_{out} = \frac{1}{2} \mathbf{w}^H \mathbf{R}_{xx} \mathbf{w} \right) \quad \text{s.t.} \quad \mathbf{w}^H \mathbf{a}(\theta) = 1 \quad (3)$$

where R_{xx} is the correlation matrix, w is the weight vector, and $a(\theta)$ is the steering vector for angle θ . The angular spectrum is given by:

$$P_{CP}(\theta) = \frac{1}{\mathbf{a}^H(\theta) \mathbf{R}_{xx}^{-1} \mathbf{a}(\theta)} \quad (4)$$

where $P_{CP}(\theta)$ indicates the power output at angle θ , with peak positions in the spectrum showing target directions and peak heights reflecting wave power. The Capon algorithm acts as a spatial filter, focusing on specific directions while suppressing signals from other angles. The angle information obtained

from the Capon beamformer, combined with the range data derived from the range-FFT, is used to generate range-azimuth and range-elevation maps of the subject.

C. Feature Reduction

In the next module, in order to simplify the models and improve activity classification performance, we reduced the feature vector size before inputting it into the ML models. We compared results using 100 and 150 principal components in PCA and selected 100 components for optimal performance. PCA [18] helps to reduce noise and handle multicollinearity by transforming correlated features into uncorrelated principal components. This simplifies the model, speeds up training, and reduces the chance of overfitting. It also improves computational efficiency and model performance.

D. Activity Classification

An ML algorithm classifies each resulting feature vector into one of the predicted activity categories. Therefore, after feature reduction, we evaluated different conventional ML classifiers to recognize various activities. Detailed information about each ML algorithm is provided below. The hyperparameters of each ML algorithm were optimized using a grid search, with the specific values listed below.

- k -Nearest Neighbor (kNN) where $n_neighbors = 9$,
- Random Forest (RF) where $number_of_estimators = 100$ specifying the number of trees in the forest, and $random_state = 42$ ensures reproducibility of results by controlling the randomness during model training,
- Decision Tree (DT) where $random_state = 42$ for the purpose of reproducibility,
- Naïve Bayes (NB),
- Multi-Layer Perceptron (MLP) where the $hidden_layer_sizes = (128 \times 64)$ specifies two hidden layers with 128 and 64 neurons, respectively, $max_iteration = 300$ limits the number of training iterations, and $random_state = 42$ ensures reproducibility of the model,
- Support Vector Machine (SVM) where $probability = True$ enables probability estimates, $C = 10$ controls the trade-off between error rates, and, and $kernel = rbf$ applies the radial basis function kernel.

III. EXPERIMENTAL EVALUATION

In this section, we report the experimental evaluation of our proposed functional prototype of the system which was carried out with real-world data acquired from three subjects by FMCW radars installed in a bedroom. Therefore, in the following subsections, we explain the experimental setup and the achieved results.

A. Experimental Setup

We developed a prototype of our system using Python and its associated libraries, running on a machine equipped with an AMD Ryzen 7 6800H processor, 32 GB of RAM, and an NVIDIA GeForce RTX 3060 GPU, operating on Windows

11. Model development utilized Python 3.8.19, and Scikit-learn 1.3.2. The system was trained on data from 14 trials and subsequently tested using data from 2 additional trials.

We report the average values of the F_1 -score and accuracy. The F_1 -score, the harmonic mean of precision and recall, is presented in both weighted and macro-averaged forms. The weighted F_1 -score averages over all instances, while the macro-averaged F_1 -score is averaged across each activity class. The macro-averaged F_1 -score is a useful way to measure classification performance because it treats all classes equally, regardless of the number of instances in each class. Accuracy is calculated as the ratio of correct predictions to the total number of predictions.

B. Experimental Results

In our experiments, we assessed the performance of various ML classifiers in recognizing different set of human activities using radar-based features. The classifiers were trained and tested on reduced feature vectors derived from range-Doppler, range-azimuth, and range-elevation maps. Table II provides detailed performance metrics for each classifier.

We evaluated the system’s performance across different activity sets. Initially, we classified seven activities and then incrementally removed less significant labels to focus on primary classes. The ‘Transition’ class was removed first, followed by the ‘Empty Room’ class, and finally the ‘Lay Down on the Floor’ class. This step-by-step approach allowed us to refine the model’s performance and better assess its effectiveness for core activities.

Indeed, this classification is crucial for monitoring daily activities especially in long-term care facilities, where detecting abnormal patterns like prolonged inactivity or unexpected transitions can signal health issues. Monitoring activities also helps assess daily activity levels and prompts interventions when necessary. The system’s real-time, unobtrusive monitoring supports timely responses from caregivers and enhances the quality of care, helping elderly individuals maintain independence.

For seven activity classes, SVM achieved the highest accuracy (70.97%) and macro F_1 -score (70.41%), followed by MLP with strong performance in macro F_1 -score (65.85%) and accuracy (68.71%) still lagged behind SVM in accuracy.

Reducing the number of classes to six improved all models’ performance. This indicates that reducing the number of activities simplifies the classification task, benefiting most models. However, SVM still led in accuracy (76.34%), with MLP showing significant gains in both weighted (75.40%) and macro F_1 -scores (75.58%). Additionally, based on the SVM confusion matrices in Table. III and Table IV, the average correct classification rate is over 73% on average considering all seven activity classes and exceeds 81% on average for the six activity classes, respectively. This suggests that SVM is most effective for recognizing a diverse set of activities within this more complex scenario.

However, with seven activity classes, there is notable confusion between similar activities, such as “Lying on the bed”

TABLE II: Comparison of F_1 -scores (%) and Accuracy (%) for different ML classifiers across varying activity sets.

Number of Activities	Metrics	ML-based Activity Classification					
		SVM	MLP	NB	DT	RF	KNN
7	Weighted F_1 -score	70.82	68.95	30.14	50.31	54.65	51.69
	Macro F_1 -score	70.41	65.85	33.41	49.57	57.15	53.41
	Accuracy	70.97	68.71	31.89	51.31	56.34	54.02
6	Weighted F_1 -score	76.28	75.40	32.13	54.41	61.16	57.85
	Macro F_1 -score	77.75	75.58	36.03	55.51	63.89	61.35
	Accuracy	76.34	75.40	34.09	55.71	62.59	59.49
5	Weighted F_1 -score	76.86	78.20	36.42	59.68	63.01	58.29
	Macro F_1 -score	79.86	80.99	42.58	61.20	66.13	63.85
	Accuracy	76.63	78.25	42.89	60.21	63.72	59.34
4	Weighted F_1 -score	88.39	89.99	68.29	76.15	74.27	72.63
	Macro F_1 -score	89.08	90.43	64.78	75.73	75.63	74.16
	Accuracy	88.80	90.28	66.78	77.36	77.15	76.17

TABLE III: Confusion matrix for the SVM classifier with seven activities, showing percentages.

		Predicted Label						
		Empty room	Enter the room and walk	Lay down on the bed	Lay down on the floor	Sit on the bed	Transitions	Sit on the chair
Actual Label	Empty room	91.74	1.25	5.45	1.56	0.0	0.0	0.0
	Enter the room and walk	0.0	97.60	0.56	1.12	0.48	0.24	0.0
	Lay down on the bed	0.45	0.26	89.75	1.75	0.19	7.59	0.00
	Lay down on the floor	8.90	3.09	30.12	56.64	0.13	0.33	0.79
	Sit on the bed	0.0	3.67	0.99	0.0	76.59	18.76	0.0
	Transitions	0.0	9.65	4.51	2.38	18.3	55.39	9.77
	Sit on the chair	27.05	0.25	11.54	9.38	0.08	0.17	51.54

TABLE IV: Confusion matrix of the SVM in classifying six activities, showing percentages.

		Predicted Label					
		Empty room	Enter the room and walk	Lay down on the bed	Lay down on the floor	Sit on the bed	Sit on the chair
Actual Label	Empty room	91.59	1.40	4.98	2.02	0.00	0.00
	Enter the room and walk	0.08	98.40	0.32	0.88	0.32	0.00
	Lay down on the bed	0.52	0.52	96.11	1.69	0.17	0.00
	Lay down on the floor	8.54	2.83	28.42	58.90	0.13	1.18
	Sit on the bed	0.00	6.35	0.99	0.00	92.52	0.14
	Sit on the chair	27.55	0.17	8.55	9.13	0.00	54.61

and “Lying on the floor”. Additionally, natural movements occurring during activities like “Lying on the bed” or “Sitting on the bed” can lead to misclassification with the “Transition” class. Furthermore, brief periods without specific movements may cause confusion between the “Empty room” and “Lying on the floor” or “Sitting on the chair”. When the “Transition” class is removed, reducing the classification to six activity classes, the classification performance becomes more balanced

across the remaining activities. However, challenges persist in distinguishing between similar activities, such as “Lying on the bed” and “Lying on the floor”.

With five activity classes, MLP excelled, achieving the highest macro F_1 -score (80.99%) and accuracy (78.25%), indicating its effectiveness in fewer activity scenarios. SVM also performed well, particularly in macro F_1 -score (79.86%). Table V which illustrates MLP confusion matrix, highlights the classifier’s robustness in distinguishing between the reduced set of activities with the average correct classification rate is over 82% for all five activity classes, particularly in recognizing “Entering the room and walking”, “Lay down on the bed”, and “Sit on the bed.”

TABLE V: Confusion matrix of the MLP in classifying five activities, showing percentages.

		Predicted Label				
		Enter the room and walk	Lay down on the bed	Lay down on the floor	Sit on the bed	Sit on the chair
Actual Label	Enter the room and walk	97.04	0.56	1.60	0.72	0.08
	Lay down on the bed	0.52	94.68	2.79	1.82	0.19
	Lay down on the floor	2.86	28.91	63.40	1.77	3.06
	Sit on the bed	3.10	0.42	0.00	96.33	0.14
	Sit on the chair	0.66	15.60	18.09	1.00	64.65

For four classes, MLP continued to lead with the highest macro F_1 -score (90.43%) and accuracy (90.28%). Its confusion matrix for four activities, depicted in Table VI, exceeds an 89% average correct classification rate, which highlights the strong performance of the MLP in simplified classification tasks.

DT and SVM also showed high scores, reflecting their robust capabilities across different levels of complexity. The

TABLE VI: Confusion matrix of the MLP in classifying five activities, showing percentages.

		Predicted Label			
		Enter the room and walk	Lay down on the bed	Sit on the bed	Sit on the chair
Actual Label	Enter the room and walk	98.64	0.64	0.56	0.16
	Lay down on the bed	0.32	97.21	2.27	0.19
	Sit on the bed	2.54	1.13	96.19	0.14
	Sit on the chair	0.83	28.13	1.74	69.29

confusion between “sitting on a chair” and “lying down on the floor” can likely be attributed to similar body positions and movements, as well as an unbalanced dataset. Both activities can produce overlapping radar signatures, especially when considering the radar’s angle and the minimal movement involved in sitting and lying down. Additionally, the dataset used contains less data for the “sitting” activity compared to other activities, which may have hindered the model’s ability to accurately learn and distinguish the unique features of sitting from those of lying down. Balancing the dataset and incorporating more diverse training data could help mitigate this issue.

In summary, SVM excels by maximizing the margin between classes, especially with overlapping features, and performs well on smaller datasets due to reduced overfitting. MLP is effective with fewer classes by learning complex patterns and benefits from removing ambiguous classes like “Transition”. However, SVM faces challenges with large, noisy datasets, while MLP requires substantial computational resources, careful hyperparameter tuning, and is prone to overfitting with limited or less diverse data.

IV. CONCLUSION

In this paper, we designed and developed a HAR framework using mmWave FMCW radar focusing on the system architecture, including the radar setup, preprocessing pipeline, multi-dimensional feature maps, and intricate, less-studied human activities. The framework classifies activities into seven categories by capturing essential motion and spatial details in 3D data vectors, which balance computational efficiency and accuracy. Unlike conventional image-based radar data processing, our approach processes raw radar data into structured feature maps, emphasizing both temporal and spatial characteristics of human activities. The system was experimentally validated using a dataset collected in a realistic environment, with MLP and SVM classifiers achieving promising recognition rates compared to other conventional ML classifiers. SVM handled complex, overlapping features effectively, while MLP excelled with less ambiguous activities, highlighting the importance of classifier selection based on data characteristics. Despite

its effectiveness, challenges remain in distinguishing highly similar activities and managing periods of inactivity. Future work will focus on lightweight deep learning models, such as Long Short-Term Memory (LSTM) networks or Convolutional Neural Networks (CNNs), to improve accuracy and adaptability, along with expanding activity categories and testing in more complex conditions for enhanced suitability in long-term care and ambient-assisted living environments.

REFERENCES

- [1] Y. Zhao, H. Zhou, S. Lu, Y. Liu, X. An, and Q. Liu, “Human activity recognition based on non-contact radar data and improved pca method,” *Applied Sciences (Switzerland)*, vol. 12, 7 2022.
- [2] A. Ferrari, D. Micucci, M. Mobilio, and P. Napoletano, “Deep learning and model personalization in sensor-based human activity recognition,” *Journal of Reliable Intelligent Environments*, vol. 9, pp. 27–39, 3 2023.
- [3] P. Rashidi and A. Mihailidis, “A survey on ambient-assisted living tools for older adults,” *IEEE journal of biomedical and health informatics*, vol. 17, no. 3, pp. 579–590, 2012.
- [4] F. J. Abdu, Y. Zhang, and Z. Deng, “Activity classification based on feature fusion of fmcw radar human motion micro-doppler signatures,” *IEEE Sensors Journal*, vol. 22, pp. 8648–8662, 5 2022.
- [5] S. Zolfaghari, S. Suravee, D. Riboni, and K. Yordanova, “Sensor-based locomotion data mining for supporting the diagnosis of neurodegenerative disorders: A survey,” *ACM Computing Surveys*, vol. 56, 8 2023.
- [6] S. Mirjalali, S. Peng, Z. Fang, C.-H. Wang, and S. Wu, “Wearable sensors for remote health monitoring: Potential applications for early diagnosis of covid-19,” *Advanced materials technologies*, vol. 7, no. 1, p. 2100545, 2022.
- [7] H. Abedi, “Use of millimeter wave fmcw radar to capture gait parameters,” *American Journal of Biomedical Science & Research*, vol. 6, pp. 122–123, 11 2019.
- [8] H. Abedi, A. Ansariyan, P. P. Morita, A. Wong, J. Boger, and G. Shaker, “Ai-powered noncontact in-home gait monitoring and activity recognition system based on mm-wave fmcw radar and cloud computing,” *IEEE Internet of Things Journal*, vol. 10, pp. 9465–9481, 6 2023.
- [9] J.-M. Muñoz-Ferreras, Z. Peng, R. Gómez-García, and C. Li, “Review on advanced short-range multimode continuous-wave radar architectures for healthcare applications,” *IEEE Journal of Electromagnetics, RF and Microwaves in Medicine and Biology*, vol. 1, no. 1, pp. 14–25, 2017.
- [10] K. Papadopoulos and M. Jelali, “A comparative study on recent progress of machine learning-based human activity recognition with radar,” *Applied Sciences*, vol. 13, p. 12728, 11 2023.
- [11] S. Ahmed, K. D. Kallu, S. Ahmed, and S. H. Cho, “Hand gestures recognition using radar sensors for human-computer-interaction: A review,” pp. 1–24, 2 2021.
- [12] “Bgt60tr13c - xensiv™ 60ghz radar sensor for advanced sensing,” <https://www.infineon.com/cms/en/product/sensor/radar-sensors/radar-sensors-for-iot/60ghz-radar/bgt60tr13c/>, 2023.
- [13] Z. Peng and C. Li, “Portable microwave radar systems for short-range localization and life tracking: A review,” 3 2019.
- [14] S. Jardak, T. Kiuru, M. Metso, P. Pursula, J. Häkli, M. Hirvonen, S. Ahmed, and M.-S. Alouini, “Detection and localization of multiple short range targets using fmcw radar signal,” in *2016 Global Symposium on Millimeter Waves (GSMM) & ESA Workshop on Millimetre-Wave Technology and Applications*, 2016, pp. 1–4.
- [15] X. Zeng, H. S. L. Báruson, and A. Sundvall, “Walking step monitoring with a millimeter-wave radar in real-life environment for disease and fall prevention for the elderly,” *Sensors*, vol. 22, no. 24, p. 9901, 2022.
- [16] C. Will, P. Vaishnav, A. Chakraborty, and A. Santra, “Human target detection, tracking, and classification using 24-ghz fmcw radar,” *IEEE Sensors Journal*, vol. 19, no. 17, pp. 7283–7299, 2019.
- [17] H. Abedi, J. Boger, P. P. Morita, A. Wong, and G. Shaker, “Hallway gait monitoring using novel radar signal processing and unsupervised learning,” *IEEE Sensors Journal*, vol. 22, pp. 15 133–15 145, 8 2022.
- [18] A. Maćkiewicz and W. Ratajczak, “Principal components analysis (pca),” *Computers & Geosciences*, vol. 19, no. 3, pp. 303–342, 1993.